

REPORT DOCUMENTATION PAGE			Form Approved OMB NO. 0704-0188		
<p>The public reporting burden for this collection of information is estimated to average 1 hour per response, including the time for reviewing instructions, searching existing data sources, gathering and maintaining the data needed, and completing and reviewing the collection of information. Send comments regarding this burden estimate or any other aspect of this collection of information, including suggestions for reducing this burden, to Washington Headquarters Services, Directorate for Information Operations and Reports, 1215 Jefferson Davis Highway, Suite 1204, Arlington VA, 22202-4302. Respondents should be aware that notwithstanding any other provision of law, no person shall be subject to any penalty for failing to comply with a collection of information if it does not display a currently valid OMB control number.</p> <p>PLEASE DO NOT RETURN YOUR FORM TO THE ABOVE ADDRESS.</p>					
1. REPORT DATE (DD-MM-YYYY) 22-02-2017		2. REPORT TYPE Final Report		3. DATES COVERED (From - To) 1-Aug-2013 - 31-Jul-2015	
4. TITLE AND SUBTITLE Final Report: Equipment for Developing Frequency Agile Plasmonic Antennas and Sensors			5a. CONTRACT NUMBER W911NF-13-1-0252		
			5b. GRANT NUMBER		
			5c. PROGRAM ELEMENT NUMBER 611103		
6. AUTHORS Xiaoqin Li			5d. PROJECT NUMBER		
			5e. TASK NUMBER		
			5f. WORK UNIT NUMBER		
7. PERFORMING ORGANIZATION NAMES AND ADDRESSES University of Texas at Austin 101 East 27th Street Suite 5.300 Austin, TX 78712 -1532			8. PERFORMING ORGANIZATION REPORT NUMBER		
9. SPONSORING/MONITORING AGENCY NAME(S) AND ADDRESS (ES) U.S. Army Research Office P.O. Box 12211 Research Triangle Park, NC 27709-2211			10. SPONSOR/MONITOR'S ACRONYM(S) ARO		
			11. SPONSOR/MONITOR'S REPORT NUMBER(S) 63379-EL-RIP.2		
12. DISTRIBUTION AVAILABILITY STATEMENT Approved for Public Release; Distribution Unlimited					
13. SUPPLEMENTARY NOTES The views, opinions and/or findings contained in this report are those of the author(s) and should not be construed as an official Department of the Army position, policy or decision, unless so designated by other documentation.					
14. ABSTRACT We requested equipment to advance projects funded by a regular ARO grant ARO W911NF-11-1-0447. The scientific goal is to build novel frequency agile plasmonic antennas and sensors. With increasing demand to faster and smaller electronic and photonic devices, plasmonic technology which has promising approach to control light at length scale well below the optical diffraction limit has emerged. The small length scale of plasmonic device, however, brings serious challenges in assembling, designing, and characterizing. The objective of this proposal is to develop an integrated method for assembly and characterization of individual nanostructures to explore new design					
15. SUBJECT TERMS equipment, plasmonic sensor, and nanophotonics					
16. SECURITY CLASSIFICATION OF:			17. LIMITATION OF ABSTRACT UU	15. NUMBER OF PAGES	19a. NAME OF RESPONSIBLE PERSON Xiaoqin Li
a. REPORT UU	b. ABSTRACT UU	c. THIS PAGE UU			19b. TELEPHONE NUMBER 512-471-2063

## Report Title

Final Report: Equipment for Developing Frequency Agile Plasmonic Antennas and Sensors

### ABSTRACT

We requested equipment to advance projects funded by a regular ARO grant ARO W911NF-11-1-0447. The scientific goal is to build novel frequency agile plasmonic antennas and sensors. With increasing demand to faster and smaller electronic and photonic devices, plasmonic technology which has promising approach to control light at length scale well below the optical diffraction limit has emerged. The small length scale of plasmonic device, however, brings serious challenges in assembling, designing, and characterizing. The objective of this proposal is to develop an integrated method for assembly and characterization of individual nanostructures, to explore new design principles for plasmonic photonic devices, and to demonstrate prototypical devices to verify the effectiveness of both theoretical simulation and experimental approaches.

---

**Enter List of papers submitted or published that acknowledge ARO support from the start of the project to the date of this printing. List the papers, including journal references, in the following categories:**

**(a) Papers published in peer-reviewed journals (N/A for none)**

<u>Received</u>	<u>Paper</u>
02/22/2017	1 Jinwei Shi, Francesco Monticone, Sarah Elias, Yanwen Wu, Daniel Ratchford, Xiaoqin Li, Andrea Alu. Modular assembly of optical nanocircuits, Nature Communications, ( ): 3896. doi:
<b>TOTAL:</b>	<b>1</b>

**Number of Papers published in peer-reviewed journals:**

---

**(b) Papers published in non-peer-reviewed journals (N/A for none)**

<u>Received</u>	<u>Paper</u>
<b>TOTAL:</b>	

**Number of Papers published in non peer-reviewed journals:**

---

**(c) Presentations**

Number of Presentations: 0.00

---

**Non Peer-Reviewed Conference Proceeding publications (other than abstracts):**

Received      Paper

**TOTAL:**

Number of Non Peer-Reviewed Conference Proceeding publications (other than abstracts):

---

**Peer-Reviewed Conference Proceeding publications (other than abstracts):**

Received      Paper

**TOTAL:**

Number of Peer-Reviewed Conference Proceeding publications (other than abstracts):

---

**(d) Manuscripts**

Received      Paper

**TOTAL:**

Number of Manuscripts:

---

**Books**

Received      Book

**TOTAL:**

Received

Book Chapter

**TOTAL:**

---

**Patents Submitted**

---

**Patents Awarded**

---

**Awards**

The PI received a Humboldt fellowship and was elected to APS fellowship

---

---

**Graduate Students**

NAME

PERCENT SUPPORTED

**FTE Equivalent:**

**Total Number:**

---

**Names of Post Doctorates**

NAME

PERCENT SUPPORTED

**FTE Equivalent:**

**Total Number:**

---

**Names of Faculty Supported**

NAME

PERCENT SUPPORTED

**FTE Equivalent:**

**Total Number:**

---

**Names of Under Graduate students supported**

NAME

PERCENT SUPPORTED

**FTE Equivalent:**

**Total Number:**

### Student Metrics

This section only applies to graduating undergraduates supported by this agreement in this reporting period

The number of undergraduates funded by this agreement who graduated during this period: ..... 0.00

The number of undergraduates funded by this agreement who graduated during this period with a degree in science, mathematics, engineering, or technology fields:..... 0.00

The number of undergraduates funded by your agreement who graduated during this period and will continue to pursue a graduate or Ph.D. degree in science, mathematics, engineering, or technology fields:..... 0.00

Number of graduating undergraduates who achieved a 3.5 GPA to 4.0 (4.0 max scale):..... 0.00

Number of graduating undergraduates funded by a DoD funded Center of Excellence grant for Education, Research and Engineering:..... 0.00

The number of undergraduates funded by your agreement who graduated during this period and intend to work for the Department of Defense ..... 0.00

The number of undergraduates funded by your agreement who graduated during this period and will receive scholarships or fellowships for further studies in science, mathematics, engineering or technology fields: ..... 0.00

### Names of Personnel receiving masters degrees

NAME

**Total Number:**

### Names of personnel receiving PHDs

NAME

**Total Number:**

### Names of other research staff

NAME

PERCENT SUPPORTED

**FTE Equivalent:**

**Total Number:**

### Sub Contractors (DD882)

### Inventions (DD882)

### Scientific Progress

see attachment

### Technology Transfer

## **Final Report for ARO grant W911NF-13-1-0252**

### **Equipment for Developing Frequency Agile Plasmonic Antennas and Sensors**

PI: Xiaoqin (Elaine) Li

Physics department, the University of Texas-Austin, Austin, TX, 78712.

Tel: 512-471-2063; Fax: 512-471-1005; Email: elaineli@physics.utexas.edu

#### **Scientific Progress Report:**

##### **A. Objective**

We requested equipment to advance projects funded by a regular ARO grant ARO W911NF-11-1-0447. The scientific goal is to build novel frequency agile plasmonic antennas and sensors. With increasing demand to faster and smaller electronic and photonic devices, plasmonic technology which has promising approach to control light at length scale well below the optical diffraction limit has emerged. The small length scale of plasmonic device, however, brings serious challenges in assembling, designing, and characterizing. The objective of this proposal is to develop an integrated method for assembly and characterization of individual nanostructures, to explore new design principles for plasmonic photonic devices, and to demonstrate prototypical devices to verify the effectiveness of both theoretical simulation and experimental approaches.

##### **B. The importance of the proposed research**

We propose to use nanomanipulation method, which is based on atomic force microscopy (AFM), to assemble plasmonic nanophotonic device in a reconfigurable manner and to characterize these devices using optical dark-field scattering spectra. In addition to the development of the methodology, the expected outcome of the project includes the demonstration of a photonic circuit consisting of both metallic and dielectric nanoparticles as described in details below.

##### **C. Accomplishment**

We experimentally demonstrated that circuit concepts can be used to model photonic components, extending the powerful concept of modular and lumped elements from electronics to photonics. This work was published in Nature Communication.

We employed small colloidal metallic and dielectric nanoparticles (NPs), ideal platforms to translate these concepts to nanophotonic systems. With optical nanocircuit concepts, we are able to control the intrinsic optical impedance of NPs by their geometry and material composition. This impedance is defined as the ratio of the local potential difference  $V=|E| \cdot L$  and the flux of displacement current  $I_d=-i\omega|E|S$  through the NP, where  $E$  is the local electric field vector,  $L$  is the NP length along the electric field,  $\omega$  is the frequency of operation,  $\epsilon$  is the NP dielectric constant and  $S$  is its transverse cross-section. It follows that a dielectric NP with  $\text{Re}(\epsilon) > 0$  behaves as a nanocapacitor, while a metallic NP with  $\text{Re}(\epsilon) < 0$  acts as a nanoinductor. Ohmic loss in the materials takes the role of a nanoresistor.

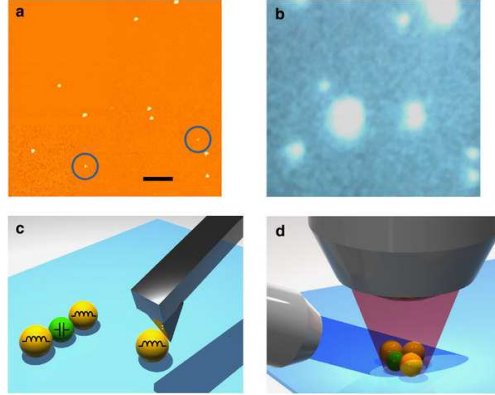
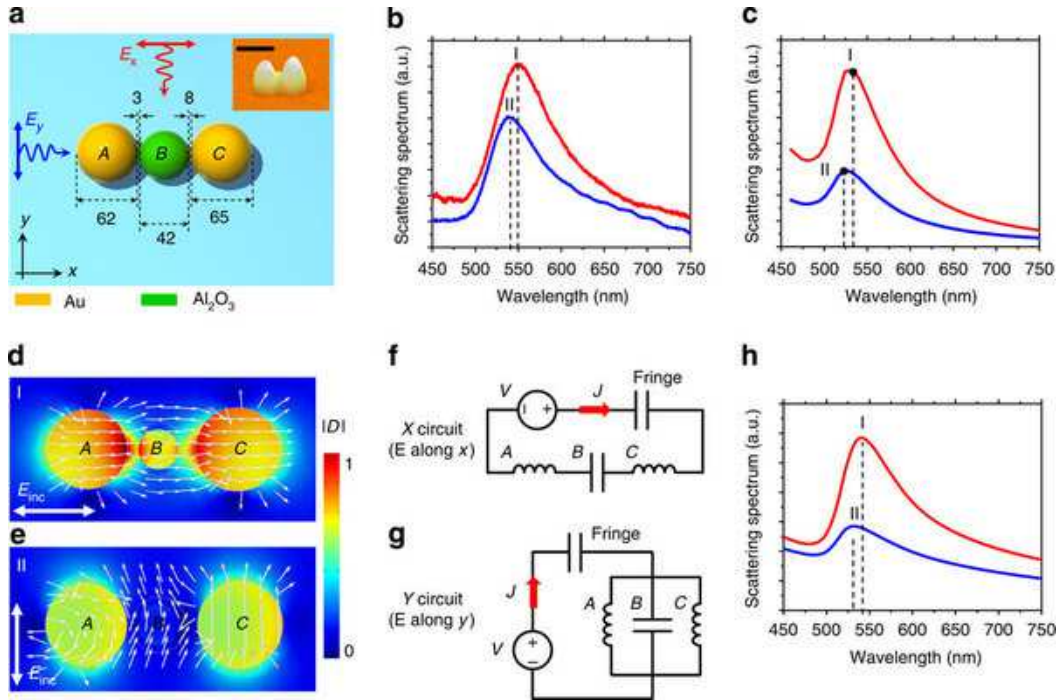


Figure 1: **Assembly and characterization of a modular optical nanocircuit.** (a) AFM and (b) dark-field scattering images of plasmonic and dielectric NPs randomly distributed on a glass substrate. Only Au NPs yield strong scattering signals. Scale bar, 3  $\mu\text{m}$ . The NPs enclosed in circles in a are missing in b, thereby identifying them as dielectric NPs. (c) Illustration of AFM nanomanipulation as a way to dynamically assemble complex optical nanocircuits from independent optical inductors (plasmonic NPs, yellow) and capacitors (dielectric NPs, green). (d) Schematic representation of our dark-field scattering measurements. Light impinges at an incidence angle of 60 degrees and the scattering signal is collected along the substrate normal.

In this experiment, gold NPs ( $\sim 60$  nm in diameter) and  $\text{Al}_2\text{O}_3$  NPs ( $\sim 45$  nm in diameter) were dispersed on a glass substrate. The AFM image of the sample (Fig. 1a) allowed us to locate each NP but did not distinguish between different NP types without ambiguity. Then we mapped the same area using optical dark-field microscopy, from which only scattering signals from Au NPs were detectable (Fig. 1b). Correlating the AFM and optical scattering images allowed us to differentiate metallic NPs (nanoinductors) from dielectric NPs (nanocapacitors) with certainty. By measuring the scattering from each NP, we detected differences in the scattering spectra because of slight variations in NP shape and size. We then picked a few chosen NPs with the desired impedance and assembled them to produce more complex connections (Fig. 1c) using the AFM tip. Finally, dark-field scattering measurements, shown schematically in Fig. 1d, were used to confirm the functionality of the nanoclusters by comparing the measured scattering spectra with the predicted nanocircuit response.

We first consider a three-particle nanocircuit consisting of a dielectric  $\text{Al}_2\text{O}_3$  NP sandwiched between two Au NPs, as shown in Fig. 2a. The measured scattering spectra from this nanocluster using s-polarized light are shown in Fig. 2b, with the incident electric field either perpendicular to the NP array (Y-circuit, blue line) or along it (X-circuit, red line). Owing to the anisotropy of this nanocluster, the optical response exhibits a spectral shift dependent on the direction of the impinging field relative to the NP array. A red shift in resonant wavelength is expected for the X-circuit (Fig. 2b), which agrees with full-wave simulations (Fig. 2c). Figure 2d,e shows the corresponding simulated displacement vector distributions at the two resonant wavelengths:  $\lambda=532$  nm for incident electric field parallel to the x axis (Fig. 2d) and  $\lambda=524$  nm for electric field along the y axis (Fig. 2e). Similar to a conventional electronic circuit, the intrinsic nanoinductance of the gold NPs is not affected by other components in the circuit.

On the basis of the different electric displacement field distributions (Fig. 2d,e), two circuits with different connections among the elements (Fig. 2f,g) account for the change in the scattering spectra. The three nanocircuit elements are connected in series (X-circuit in Fig. 2f) for incident electric field polarized along the axis of the NP cluster, since this excitation ensures the continuity of the displacement current across the cluster, as confirmed by our simulations in Fig. 2d. In conventional circuit theory, the number of independent reactive elements determines the order of a filter. Accordingly, the X-circuit (Fig. 2f) realizes a second order filter, which is an LC circuit formed by the series combination of an inductor (the Au NPs) and a capacitor (determined by the  $\text{Al}_2\text{O}_3$  NP and the fringing fields). Conversely, for incident electric field perpendicular to the axis of the NP cluster (Fig. 2e), each element experiences the same potential difference (that is, voltage), leading to a parallel connection between them. This Y-circuit (Fig. 2g) forms a third order nanofilter, in which the fringe capacitance is connected in series to the parallel of the Au NP inductors and the  $\text{Al}_2\text{O}_3$  NP capacitor. The scattering spectra predicted by our circuit model (Fig. 2h) are indeed quantitatively consistent with the measured and simulated spectra for both X- and Y-circuits (Fig. 2b,c). By realizing different circuit configurations controlled by the direction of the



**Figure 2: Second and third order lumped nanofilters.** (a) AFM image and geometry of a 3-NP cluster composed of an  $\text{Al}_2\text{O}_3$  NP sandwiched between two AuNPs. All dimensions are in nanometres. Scale bar, 100 nm. (b) Dark-field scattering measurements for s-polarized light exciting the nanocircuit with the electric field along x (red line) or y (blue). (c) Corresponding full-wave simulations with electric field along x (red line) or y (blue). (d,e) Simulated electric displacement field distributions and field vectors at the resonance wavelengths for the two incidence directions:  $\lambda=532$  nm (d) and  $\lambda=524$  nm (e). (f,g) Thevenin nanocircuit models of second order and third order lumped nanofilters. (h) Corresponding circuit theory predictions: X-circuit (red line) and Y-circuit (blue).



excitation field, we are able to experimentally prove the design and operation of optical stereo-circuits, which do not have a counterpart in the electronic realm.

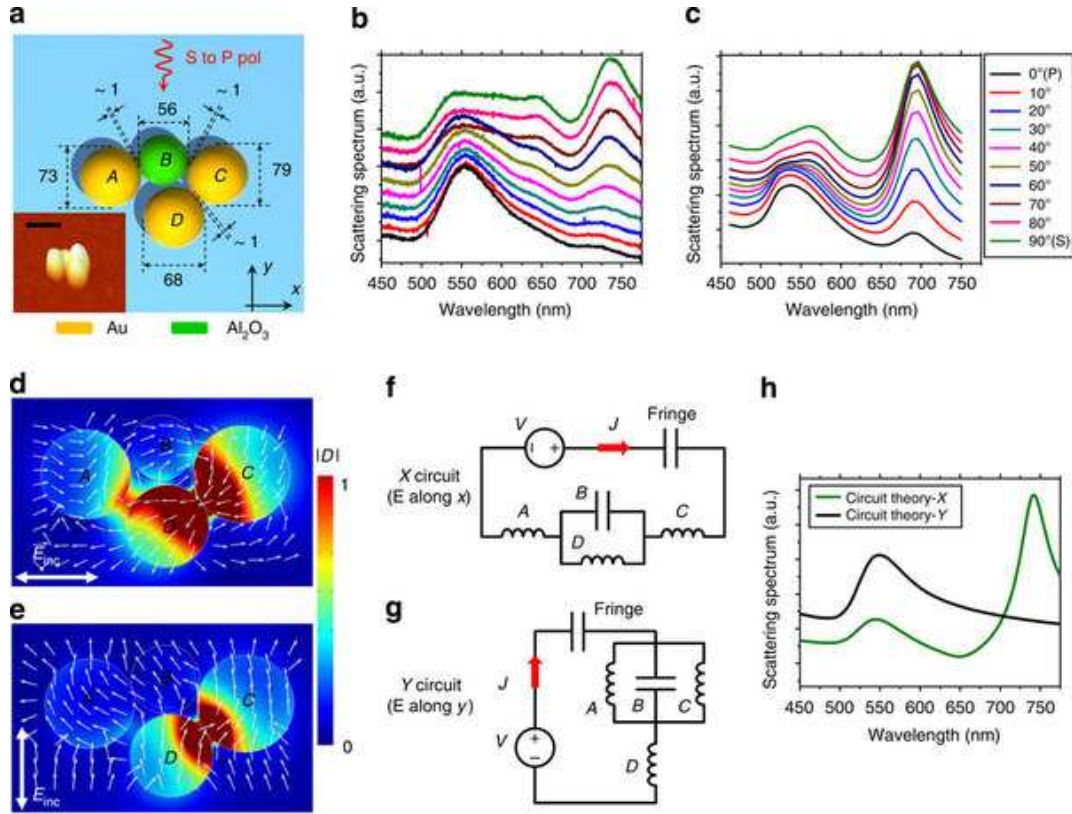


**Figure 3: A fourth order lumped nanofilter.**(a) AFM image and geometry of a 4-NP complex nanocircuit composed of three Au NPs and one Al<sub>2</sub>O<sub>3</sub>NP. All dimensions are in nanometres. Scale bar, 100 nm. (b) Dark-field scattering measurements for polarization rotating from s to p; (c) corresponding full-wave simulations. Curves in b,c have been shifted vertically to facilitate comparisons. (d,e) Simulated electric displacement field distributions and field vectors for polarizations parallel (d) and orthogonal (e) to the array axis, at the  $\lambda=688$  nm. (f,g) Thevenin nanocircuit models. (h) Corresponding circuit theory predictions for the two orthogonal polarizations.

Then we further add another metallic NP below the previous nanocircuit design, as illustrated in Fig. 3a. The scattering measurements shown in Fig. 3b were taken with incident light direction fixed while gradually changing the polarization from p to s. Our experiments (Fig. 3b) agree well with full-wave simulations (Fig. 3c). Shown in Fig. 3d,e are the simulated displacement vector distributions at the longer wavelength resonance ( $\lambda=688$  nm), for polarizations parallel (Fig. 3d) and orthogonal (Fig. 3e) to the array, highlighting the polarization-dependent interaction among NPs. Even in this more complex configuration, the electric displacement vector distributions fully support the circuit models reported in Fig. 3f,g, which correspond to fourth order nano-filters. This example shows that we can quantitatively control the spectral response by connecting an additional nanoinductor. More specifically, we have been able to add a new zero and/or pole to

the scattering response by adding an independent reactive element to the circuit of Fig. 2. Rather than modeling a distributed photonic system with an equivalent circuit, our work shows that it is actually possible to synthesize photonic circuit functionality by assembling modular lumped elements.

We would like to emphasize the key message of this work: the nanocircuit paradigm provides an unmatched degree of simplicity to control and tailor the optical response of rather complex nanophotonic structures. Remarkably, the impedance of each nanosphere remains independent of the cluster geometry and surrounding environment in all the circuits we have demonstrated, starting from the isolated NP to the complex fourth order nanocircuit. In other words, each NP carries inherent optical impedance, which is a property of the particle itself, allowing us to modularize its response and combine it in complex configurations. To the best of our knowledge, this work represented the first reconfigurable photonic circuit at the time it was reported.

#### **D. Publication in peer-reviewed journals**

1. J. Shi\*, S. Elias\*, F. Monticone\*, Y. Wu, D. Ratchford, X. Li, and A. Alù, "Modular Assembly of Optical Nanocircuits," *Nature Communications*, Vol. 5, No. 3896, May 29, 2014.